

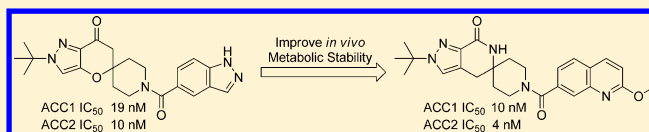
Spirolactam-Based Acetyl-CoA Carboxylase Inhibitors: Toward Improved Metabolic Stability of a Chromanone Lead Structure

David A. Griffith, Robert L. Dow, Kim Huard,* David J. Edmonds, Scott W. Bagley, Jana Polivkova, Dongxiang Zeng, Carmen N. Garcia-Irizarry, James A. Southers, William Esler, Paul Amor, Kathrine Loomis, Kirk McPherson, Kevin B. Bahnck, Cathy Préville, Terece Banks, Dianna E. Moore, Alan M. Mathiowetz, Elnaz Menhaji-Klotz, Aaron C. Smith, Shawn D. Doran, David A. Beebe, and Matthew F. Dunn

Pfizer Worldwide Research and Development, Eastern Point Road, Groton, Connecticut 06340, United States

S Supporting Information

ABSTRACT: Acetyl-CoA carboxylase (ACC) catalyzes the rate-determining step in *de novo* lipogenesis and plays a crucial role in the regulation of fatty acid oxidation. Alterations in lipid metabolism are believed to contribute to insulin resistance; thus inhibition of ACC offers a promising option for intervention in type 2 diabetes mellitus. Herein we disclose a series of ACC inhibitors based on a spirocyclic pyrazololactam core. The lactam series has improved chemical and metabolic stability relative to our previously reported pyrazoloketone series, while retaining potent inhibition of ACC1 and ACC2. Optimization of the pyrazole and amide substituents led to quinoline amide **21**, which was advanced to preclinical development.



■ INTRODUCTION

Type 2 diabetes mellitus (T2DM) is associated with a fundamental imbalance in lipid metabolism, and these alterations are hypothesized to contribute to the molecular pathogenesis of insulin resistance. In the insulin-resistant state, fatty acid oxidation is suppressed and the rate of hepatic *de novo* lipogenesis (DNL) is increased.¹ These alterations are believed to result in a net ectopic accumulation of lipid species in liver and skeletal muscle, which in turn have been hypothesized to contribute to the pathogenesis of insulin resistance.¹ This hypothesis is supported by the inverse relationship observed in rodent models and humans between insulin sensitivity and both hepatic² and intramyocellular³ triglyceride levels. Acetyl-CoA carboxylase (ACC) serves as a critical switch regulating the transition from lipogenic to oxidative lipid metabolism. Inhibition of ACC activity is expected to have a favorable impact on both skeletal muscle and hepatic insulin sensitivity by rebalancing fundamental alterations in lipid metabolism associated with the pathogenesis of insulin resistance. Consistent with this hypothesis, suppression of ACC activity by knockout,⁴ antisense oligonucleotides,⁵ or small molecule inhibitors⁶ has been shown to reduce tissue malonyl-CoA levels, increase fatty acid oxidation or inhibit lipogenesis, reduce triglyceride accumulation in skeletal muscle or liver or both, and improve insulin sensitivity in rodents. Consequently, pharmacologic ACC inhibitors may have utility in the treatment of T2DM.

Two isoforms of ACC (ACC1 and 2) are found in mammalian tissue. ACC1 is widely expressed, with higher levels in the liver and adipose tissue, and supplies the malonyl-CoA needed for DNL. ACC2 is associated with the

mitochondrial membrane and is responsible for regulation of fatty acid oxidation via inhibition of CPT-I mediated transport of fatty acids into the mitochondria.⁷ Thus, a dual ACC1/2 inhibitor may offer the greatest potential benefit, by simultaneously reducing lipid production and increasing lipid oxidation.

Screening of the Pfizer compound collection and subsequent structure-based drug design led to the identification of spiroketone-derived ACC inhibitors containing chromanone⁸ and then ketopyrazole cores.⁹ Optimization of the latter series led to the identification of compound **1**, a potent and balanced ACC1/2 inhibitor.¹⁰ The optimization process focused on lipophilic ligand efficiency (LipE)¹¹ as a key measure of success, which facilitated the identification of compounds with desirable pharmacokinetic properties. Compound **1** has moderate measured lipophilicity ($E \log D = 1.4$),¹² and thus low turnover in human liver microsomal incubation (HLM),¹³ good passive permeability in Ralph Russ canine kidney cells (RRCK, $P_{app} = 9.7 \times 10^{-6}$ cm/s),¹⁴ and a clean safety profile as predicted by *in vitro* assays. However, during preclinical development, ketone **1** was observed to undergo species-dependent reduction¹⁵ to the corresponding alcohol, which complicated human pharmacokinetic predictions. Furthermore, the chromanone-like spirocyclic core is prone to a base-mediated retro-Michael ring-opening reaction, which limits further chemical transformations.¹⁶ We therefore sought alternative series lacking the ketone functional group.

Received: July 8, 2013

Published: August 12, 2013



Earlier efforts to replace the ketone group had identified spirocyclic salicylamide derivatives, such as **2**,¹⁷ as modest ACC inhibitors (Figure 1).¹⁸ We reasoned that modification of the

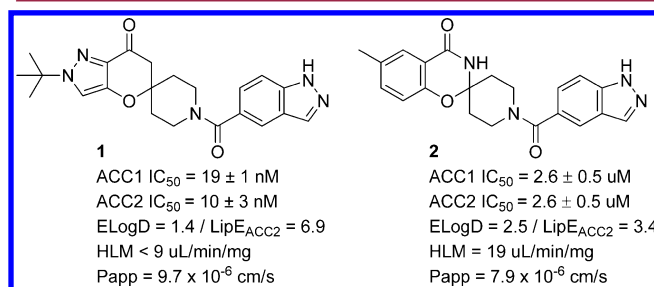


Figure 1. ACC inhibitors **1** and **2** from the spirocyclic ketone and salicylamide series. IC₅₀ values are the arithmetic mean of at least three replicates ± SEM. Each individual IC₅₀ value is generated from an 11-point dose–response curve run in triplicate. A detailed protocol can be found in the Experimental Section. LipE values are calculated using *E* log *D*.

aromatic region of **2** to the pyrazole motif of **1** would improve potency and LipE, as observed in the ketone series.⁹ The 5,6-fused spirocyclic aminal **3** was not isolated when starting from the corresponding hydroxypyrazole amide, presumably due to the angle between the hydroxyl and carboxamido substituents of the 5-membered heterocycle, which imparts unfavorable strain on the cyclic aminal. We therefore designed spiro lactam structure **4** in which the oxygen linker is replaced by a methylene group (Figure 2). Co-crystallization of the ACC

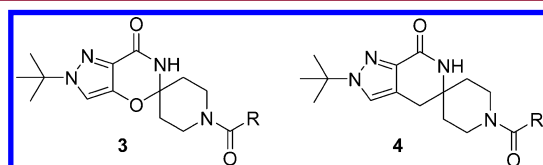


Figure 2. Lactam-based ketone replacements.

carboxyltransferase domain and **1** indicated the presence of a hydrogen bond between the ketone of **1** and the backbone of the enzyme.⁸ We hypothesized that, in addition to circumventing *in vivo* ketone reduction, replacement of the ketone with a lactam would further strengthen this hydrogen bond and thereby improve affinity for ACC. Here, we describe the discovery and optimization of this series of ACC inhibitors.

RESULTS

Synthesis. The spiro lactam cores described herein were prepared according to the general sequence shown in Scheme

1. Full details of this work have been reported separately.¹⁹ N1- and N2-substituted spirolactams were accessed from regioisomeric pyrazoles via alkylation of a piperidine carboxylic acid derivative followed by Curtius rearrangement to install the required nitrogen-based functional group. Lithiation and ring closure onto the isocyanate group forged the spirocyclic ring system, with deprotection and amidation providing the final analogs.

Pyrazole **5**¹⁹ was prepared to allow direct comparison with the ketone and aminal analogs (Figure 3). As hypothesized, the

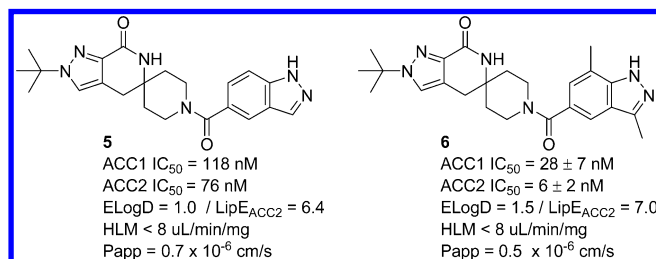


Figure 3. Spirolactam ACC inhibitors.²¹ The synthesis of **5** has been previously reported.¹⁹

t-butylpyrazole system in **5** significantly improved LipE compared with aminal **2**, where improved potency coincided with reduced lipophilicity. Although we had hypothesized that the increased H-bond acceptor strength of the amide carbonyl might improve ACC affinity, the reduced LipE of **5** compared with ketone **1** suggested that the increased desolvation penalty for the amide versus the ketone was a dominating effect and that further optimization was needed.

The low measured lipophilicity of **5** relative to the ketone series suggested that small lipophilic substituents could be added to improve potency without adversely increasing HLM metabolism. The 3,7-dimethylindazole “tail” group, which was consistently among the most potent in related series,^{8,9} was coupled with the lactam core (Figure 3). The resulting analog **6** had improved potency and LipE, but was found to be a time-dependent inhibitor of CYP3A4,²⁰ likely due to oxidative metabolism of the methyl substituents. Both compounds suffered from poor passive permeability. We therefore sought to further explore the SAR of the lactam series with the goal of maintaining a balance between ACC inhibitory potency and clearance, while removing the liabilities associated with **5** and **6**.

Series Optimization. Our investigation first focused on pyrazole substitution where the synthetic sequence depicted in Scheme 1 was used to prepare the spirolactam core with different N-substituents (Table 1). Based on the knowledge gained from our previous work with similar series, the

Scheme 1. Synthesis of N1- and N2-Substituted Spirolactam Cores and Elaboration To Form Final Amides¹⁹

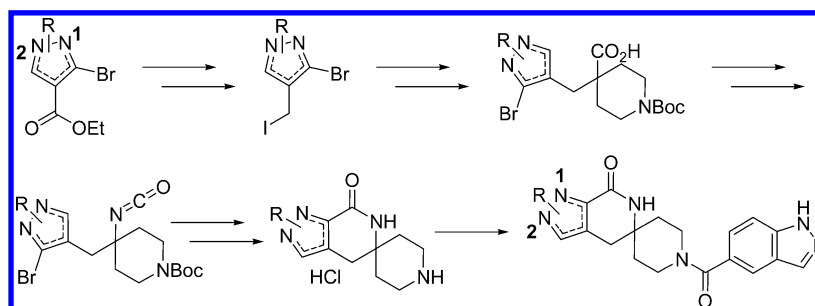
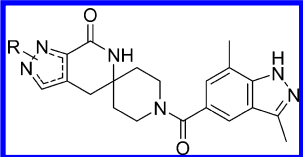
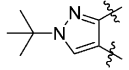
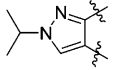
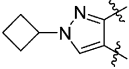
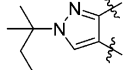
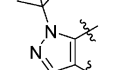
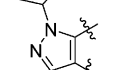
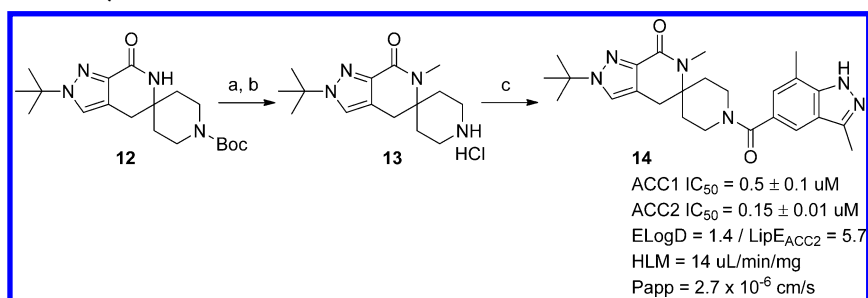


Table 1. Pyrazole SAR



Compd	Pyrazole substitution	IC ₅₀ (nM)	ELogD	LipE (ACC2)	HLM (uL/min/mg)	Papp (10 ⁻⁶ cm/s)
6		ACC1: 28 ± 7 ACC2: 6 ± 2	1.5	7.0	<8	0.5
7		ACC1: 91 ± 7 ACC2: 29 ± 3	1.1	6.7	<8	0.6
8		ACC1: 49 ± 2 ACC2: 16 ± 2	1.4 ^a	6.7 ^b	9 ^a	1.6 ^a
9		ACC1: 23 ± 1 ACC2: 4.5 ± 0.3	1.7	7.0	35	1.2
10		ACC1: 65 ± 9 ACC2: 68 ± 5	2.6	4.9	17	15
11		ACC1: 86 ± 18 ACC2: 55 ± 11	1.7	5.9	<8	7

^aCalculated values. ^bDerived from calculated *E* log *D*.

Scheme 2. Synthesis of N-Methylated Lactam 14^a

^aReagents and conditions: (a) NaH, MeI, DMF, 0 °C, 86%; (b) HCl, dioxane, 95%; (c) T3P, Et₃N, 3,7-dimethyl-1H-indazole-5-carboxylic acid, 38%. See Experimental Section for details.

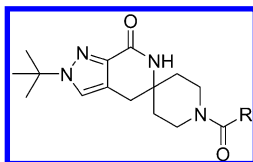
exploration was limited to small secondary or tertiary alkyl groups.⁹ As illustrated with *i*-propyl and *c*-butyl substituted pyrazoles 7 and 8, the replacement of the *t*-butyl group by a secondary group proved detrimental to potency. Compared with 6, the more lipophilic *t*-pentyl group (9) showed similar potency and permeability but higher turnover in HLM. The *t*-butyl group therefore appeared to be the optimal substituent for the N-2 lactam regioisomer.

As a way of improving passive permeability, we sought to sterically mask the inherent polarity of the lactam functionality with an adjacent alkyl group. This would increase the overall hydrophobic character of the molecule and thereby improve

permeability. The N1-substituted regioisomer was synthetically accessible with the spiro lactam core,¹⁹ and we were able to test this hypothesis. As exemplified with 10 and 11, substitution at the N1 position led to the expected higher *E* log *D* values and significantly improved permeability. However, the increased lipophilicity did not provide a corresponding increase in potency, with the lower LipE values indicating that the N-1 alkyl lactams did not inhibit ACC as efficiently as their respective N-2 counterparts (6 and 7).

An alternate strategy to increase the passive permeability of this core was to N-alkylate the lactam to eliminate an H-bond donor, and lactam 14 was prepared (Scheme 2). Although N-

Table 2. SAR on the Fused Aryl Bicyclic Portion



Compd	R	IC ₅₀ (nM)	ELogD	LipE (ACC2)	HLM (uL/min/mg)	Papp (10 ⁻⁶ cm/s)
6		ACC1: 28 ± 7 ACC2: 6 ± 2	1.5	7.0	<8	0.5
15		ACC1: 42 ± 16 ACC2: 19 ± 9	2.5	5.5	<8	1.5
16		ACC1: 17 ± 3 ACC2: 6.7 ± 0.3	1.8	6.7	<8	1.4
17		ACC1: 13 ± 4 ACC2: 6.8 ± 0.6	2.6	5.9	17	4.0
18		ACC1: 7 ± 1 ACC2: 3.0 ± 0.7	3.5	5.3	31	4.2
19		ACC1: 11 ± 5 ACC2: 5 ± 2	1.4	7.2	<8	0.8
20		ACC1: 74 ± 16 ACC2: 29 ± 7	1.6	6.2	<8	9.7

methylation led to the expected improvement in permeability, it was detrimental to ACC inhibitory potency.

Co-crystal structures of inhibitors bound to the ACC carboxyltransferase domain suggest adequate room for the methyl group, so it seems likely that the reduced affinity is the result of the increased dipole of the tertiary lactam compared with the NH lactam. Indeed, *E* log *D* was essentially unchanged by N-methylation.

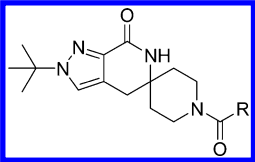
Having found the N2-*t*-butyl substituent to be the most efficient in terms of LipE, we next investigated ways to improve permeability by modifying the “tailpiece” of the molecule (R group in Table 2). To this end, a wide range of substituted 5,6-fused heteroaryl derivatives were investigated, with an emphasis on small substituents with a low risk of metabolic activation to form reactive metabolites. Potent indazoles (e.g., compounds **15** and **16**, Table 2) with good LipE and low clearance were identified; however improvements in permeability were modest. Most other 5,6-fused heteroaryl systems that were evaluated showed reduced activity. Good potency could be achieved with the more lipophilic regioisomeric chloroindoles **17** and **18**, with a resulting improvement in permeability. The increased lipophilicity was not efficiently utilized as reflected by the lower LipE values of the indole analogues and resulted in higher microsomal clearance. In an attempt to mitigate this issue, the more polar azaindole **19** was prepared. While **18** and **19** are equipotent, the increased polarity resulted in low passive permeability.

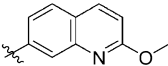
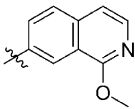
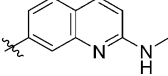
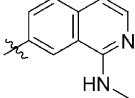
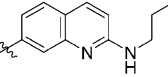
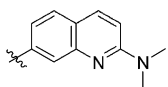
To improve permeability in the series, we sought analogues without an H-bond donor on the heterocyclic tail. In practice, replacement of the “tailpiece” with a heterocyclic 6,6-fused ring system such as **20** proved to be a breakthrough for the lactam series. Although the potency was modest, it provided a combination of good permeability and low predicted clearance.

Our design efforts in the fused 6,6-ring systems sought to combine good permeability and low turnover in HLM while optimizing potency. Unsurprisingly, the lipophilic character of naphthalene ring systems resulted in high turnover in HLM, and this scaffold was not pursued. We systematically evaluated methoxy-substituted regioisomers of quinolines and isoquinolines to identify the most efficient ACC inhibitor (data not shown). Quinoline **21** and isoquinoline **22** were identified as possessing an optimum profile (Table 3). Compounds **21** and **22** potently inhibit ACC, are stable in human liver microsomes (<8 and 12 μL/(min·mg), respectively), and possess good passive permeability (11 × 10⁻⁶ and 9.7 × 10⁻⁶ cm/s, respectively).

Solubilizing functionality was introduced to mitigate the potential for solubility-limited oral exposure of crystalline materials at higher doses. Replacement of the methoxy groups in **21** (p*K*_a = 2.2) and **22** with substituted amino groups was investigated to introduce a weakly basic site to promote solubilization in the stomach and offer the potential for salt formation (Table 3). As predicted, *N*-methyl substituted amine **23** (p*K*_a = 6.6) showed improved thermodynamic solubility (4.8 μg/mL) compared with its methoxy counterpart **21** (0.49

Table 3. SAR on the Quinoline and Isoquinoline



Compd	R	IC ₅₀ (nM)	ELogD	LipE (ACC2)	HLM (uL/min/mg)	Papp (10 ⁻⁶ cm/s)
21		ACC1: 10 ± 5 ACC2: 4 ± 1	2.2	6.5	<8	11
22		ACC1: 11 ± 2 ACC2: 4.2 ± 0.2	2.0	6.7	12	9.7
23		ACC1: 6 ± 1 ACC2: 4.2 ± 0.4	1.5	7.7	9	1.5
24		ACC1: 18 ± 3 ACC2: 6 ± 1	1.5	7.1	25	0.9
26		ACC1: 1.8 ± 0.8 ACC2: 1.7 ± 0.2	2.1	7.0	29	2.5
27		ACC1: 5 ± 1 ACC2: 2.3 ± 0.7	1.9	7.0	19	6.2

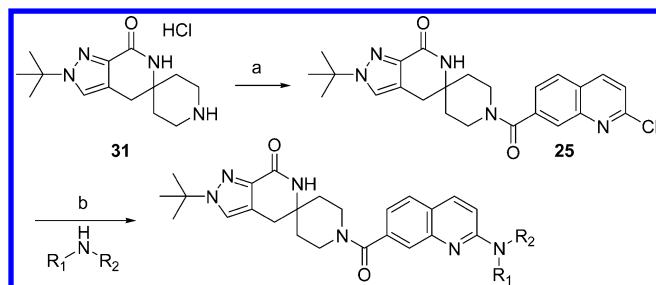
ug/mL) as determined with crystalline material at pH 1.2. Both regioisomeric methyl substituted amines (**23** and **24**) were potent ACC inhibitors; however, they possessed low permeability and low-to-moderate turnover in HLM. With the aim of improving passive permeability, analogues having a wide range of amino substituents were prepared by reaction of chloroquinoline **25** with various amines (Scheme 3). As illustrated with **26** and **27**, longer alkyl chains or disubstitution on the amino group resulted in modest improvements in passive permeability, although with poor microsomal stability (Table 3). Though a higher LipE could be achieved with amino substitution, methoxy-substituted quinoline **21** and isoquinoline

line **22** were selected as lead compounds for the project, based on their overall ADME profiles.

Compounds **21** and **22** are potent ACC inhibitors with LipEs comparable to our previous lead **1**. At 10 μ M, they showed no significant inhibition of the five major human CYP450 enzymes (CYP1A2, CYP2C8, CYP2C9, CYP2D6, and CYP3A4). Both leads were found to be selective against a set of 108 targets including various enzymes, GPCRs, ion channels, and other transporters (less than 50% inhibition at 10 μ M). In order to avoid future complications in preclinical evaluation and product development, work was carried out to find more stable crystalline forms. The more stable crystalline forms identified for **21** and **22** had reduced but likely acceptable solubility based on the good passive permeability associated with these leads (0.05 and 0.13 μ g/mL, respectively, at pH 6.5).

In Vivo Evaluation. Based on their respective profiles, **21** and **22** were advanced to pharmacokinetic evaluation. When dosed in rats at 5 mg/kg using 0.5% methylcellulose as the vehicle, **21** exhibited high oral bioavailability of 71% (C_{\max} = 403 ng/mL, AUC_{last} = 2070 ng·h/mL). As determined with a 1 mg/kg intravenous dose, **21** demonstrated moderate *in vivo* systemic clearance (29 mL/(min·kg)) and volume of distribution (1.7 L/kg). At the same doses, **22** showed lower bioavailability (F = 28%, C_{\max} = 186 ng/mL, AUC_{last} = 713 ng·h/mL) and higher clearance (41 mL/(min·kg)) compared with **21**. In acute rat pharmacodynamic studies, **21** dose-proportionally reduced DNL as measured by conversion of ¹⁴C-acetate to ¹⁴C-lipids after oral dosing, with an ED₅₀ of 1.27 mg/kg (Figure 4).

Scheme 3. Synthesis of ACC Inhibitors with Amino Substituted Quinoline Tailpieces^a



^aReagents and conditions: (a) Et₃N, HOBt, EDC, DCM, 100%; (b) substituted amine in excess, 80 °C in a sealed vial, 29–92%. See Experimental Section for details.

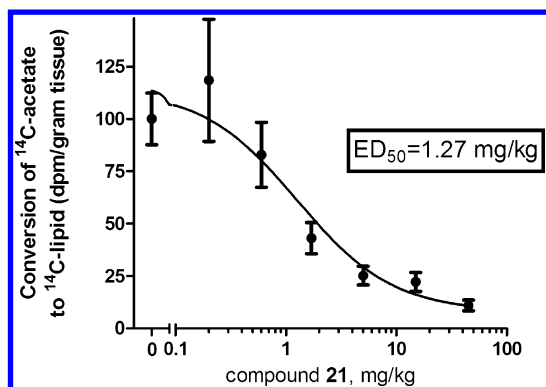


Figure 4. Graph of conversion of ^{14}C -acetate to ^{14}C -lipids (percentage vs vehicle) vs doses of **21** after oral delivery using a SEDDS formulation composed of DMSO/PEG 400/Polysorbate 80/HPMC ES LV in water. Data are the arithmetic mean of eight animals \pm SEM. A detailed protocol can be found in the Experimental Section.

CONCLUSION

In summary, the more polar spiro lactam core proved a solution to avoid *in vivo* ketone reduction observed with our previous lead **1**. Lactam **5** had good metabolic stability but decreased potency and permeability compared with **1**. Optimization of the lactam series with an aim to improve LipE, HLM stability, and passive permeability afforded potent ACC inhibitors with good *in vitro* ADME and polypharmacological profiles. Excellent oral bioavailability, moderate systemic clearance, and acceptable exposure were achieved with lead compound **21** in rat pharmacokinetic studies. In a preclinical efficacy study, oral dosing of rats with **21** resulted in potent, dose-proportional inhibition of ACC activity as measured by incorporation of ^{14}C in DNL products. Compound **21** was advanced to exploratory toxicological studies in rodents and preclinical development for T2DM.

EXPERIMENTAL SECTION

Materials and Methods. All chemicals, reagents, and solvents were purchased from commercial sources and used without further purification unless otherwise noted. ^1H NMR spectra were recorded with 400 or 500 MHz spectrometers and are reported relative to residual undeuterated solvent signals. Data for ^1H NMR spectra are reported as follows: chemical shift (δ , ppm), multiplicity, coupling constant (Hz), and integration. The multiplicities are denoted as follows: s, singlet; d, doublet; t, triplet; q, quartet; spt, septet; m, multiplet; br s, broad singlet. High-resolution mass spectrometry (HRMS) was performed via electrospray ionization (ESI) source. The system used was an Agilent 1200 DAD (G1315C), 190–400 nm scan, 4 nm slit, and Agilent 6220 MS (TOF). Silica gel chromatography was performed using a medium pressure Biotage or ISCO system and columns prepackaged by various commercial vendors including Biotage and ISCO. The terms “concentrated” and “evaporated” refer to the removal of solvent at reduced pressure on a rotary evaporator with a water bath temperature not exceeding 60 °C. All tested compounds were determined to be >95% pure by high-performance liquid chromatography (HPLC).

Preparative HPLC Conditions for Combinatorial Chemistry. Compounds prepared via combinatorial chemistry were purified by preparative HPLC using the following conditions: column, Waters Atlantis dC₁₈, 4.6 mm \times 50 mm, 5 μm ; solvents A and B are water with 0.05% TFA and MeCN with 0.05% TFA, respectively. A gradient of 5–95% of solvent B in A was used over 4 min at 2 mL/min.

In Vitro ACC1 and ACC2 Inhibition Assay. For ACC inhibition studies, test compounds were dissolved in dimethyl sulfoxide (DMSO) and serially diluted in DMSO in order to run in a 11-point dose–

response with final compound concentration ranging from 10 μM to 0.3 nM. Aliquots of 1 μL were added in replicate to 96 well plates, and an equal volume of DMSO was added to control wells. The enzyme solution was activated for 30 min at 37 °C in buffer containing 50 mM HEPES (pH 7.5), 10 mM MgCl_2 , 10 mM tripotassium citrate, 6 mM DTT, 0.75 mg/mL BSA, and 0.8 $\mu\text{g/mL}$ ACC. After a 10 min enzyme–compound preincubation, the reaction was initiated at room temperature in a fume hood by addition of the substrate solution (containing 2.4 mM acetyl-CoA, 38.4 mM KHCO_3 , 1.6 mM $\text{NaH}[^{14}\text{C}]\text{O}_3$, and 8.0 mM ATP). The final assay volume of 100 μL per well consisted of 46 mM HEPES (pH 7.5), 7.5 mM MgCl_2 , 7.5 mM tripotassium citrate, 2.8 mM DTT, 0.5 mg/mL BSA, 2.0 mM ATP, 600 μM acetyl-CoA trilitium salt, 9.6 mM potassium bicarbonate, 0.6 $\mu\text{g/mL}$ hACC1 or 2, and 0.4 mM $\text{NaH}[^{14}\text{C}]\text{O}_3$ (58 mCi/mmol). After 20 min, the reaction was terminated by the addition of a 3 N solution of hydrochloric acid (HCl) with the concomitant liberation of nonreacted NaHCO_3 as CO_2 . Plates were dried overnight at 50 °C to allow complete $^{14}\text{C}]\text{O}_2$ liberation. The following day, 30 μL of water was added to the dried wells now containing ^{14}C malonyl-CoA, followed by 95 μL of OptiPhase Supermix liquid scintillation fluid. The plates were shaken vigorously, sealed, and transferred to a Microbeta LSC luminescence counter to quantify the amount of ^{14}C in each assay well.

In Vivo DNL Study. A single dose of compound **21** was administered via oral gavage to rats 2 h into the light cycle. One hour post dose, ^{14}C -labeled acetate (0.1 $\mu\text{Ci/g}$) was administered ip. One hour post ^{14}C -acetate administration, the animals were sacrificed, and tissues were collected. Liver punches (~400 mg, bifurcated median lobe) were collected for DNL determinations as measured by ^{14}C acetate incorporation to lipid. The tissues were dissolved in NaOH (1.5 mL of 2.5 M). Following complete degradation, absolute ethanol (2.5 mL) was added to each sample, and samples were vigorously mixed. The samples were extracted with petroleum ether (4.8 mL). Following centrifugation to separate the organic and aqueous phases, the upper organic phase was removed and discarded. Concentrated HCl (0.6 mL of 12M) was added to the remaining aqueous phase and vortexed vigorously. The acidified aqueous phase was subsequently extracted with petroleum ether (4.8 mL) and then centrifuged to separate the organic and aqueous phases. The upper organic phase was collected in an appropriately sized scintillation vial. The remaining aqueous phase was extracted with petroleum ether as described above and the organic phase was combined with the previous extract. The combined organic phases were evaporated to dryness under gentle flow of nitrogen at room temperature. Compatible scintillation fluid was added to each vial, and the level of ^{14}C in the extraction was determined.

Synthesis. General Procedure A. To a solution of amine (1 equiv) in DMF (0.25 M) were added the carboxylic acid (1–3 equiv), Et_3N (3–6 equiv), and T3P (1–2 equiv). The resultant mixture was stirred for 18 h at room temperature (rt). The mixture was diluted with EtOAc and washed subsequently with water and brine. The aqueous washes were combined and extracted with additional EtOAc. The combined organic extracts were dried over Na_2SO_4 , filtered, and concentrated under reduced pressure.

General Procedure B. To a solution of the carboxylic acid (1 equiv) in DCM (0.1 M) were added DMAP (0.3 equiv), T3P (1.25 equiv), and Et_3N (2–3 equiv). The mixture was stirred for 10 min at rt before a solution of amine (1 equiv) and Et_3N (1.25 equiv) in DCM (0.1 M) was added, and the resultant mixture was stirred at rt for 18 h. A saturated aqueous solution of NaHCO_3 was added and stirred for 10 min then extracted with DCM (2 \times). The combined organic layers were dried over Na_2SO_4 , filtered, and concentrated.

General Procedure C. To a solution of the carboxylic acid (1 equiv) in DCM (0.1 M) were added the amine (1 equiv), Et_3N (3 equiv), and HATU (1 equiv). The resultant mixture was stirred at rt for 18 h. The mixture was washed with a saturated aqueous solution of NaHCO_3 and brine. The organic layer was dried over Na_2SO_4 , filtered, and concentrated.

General Procedure D. To a suspension of carboxylic acid (1 equiv) in DMF (0.3 M) were added the amine (1 equiv), EDC (1–1.5 equiv),

and HOBt (1–1.5 equiv) followed by Et₃N (3–4 equiv). The reaction was warmed to 50 °C and stirred at that temperature for 3.5 h. The reaction was allowed to cool to rt and partitioned between water and DCM. The aqueous layer was extracted with further DCM (3×), and the combined organic solutions were dried over Na₂SO₄, filtered, and concentrated.

1'-(1H-Indazole-5-carbonyl)-6-methylspiro[benzo[e][1,3]oxazine-2,4'-piperidin]-4(3H)-one (2). The title compound was prepared from 6-methylspiro[1,3-benzoxazine-2,4'-piperidin]-4(3H)-one hydrochloride salt (**28**)²² (35 mg, 0.15 mmol), 1H-indazole-5-carboxylic acid (**29**) (86 mg, 0.45 mmol), Et₃N (73 µL, 0.52 mmol), and T3P (0.15 mL, 50% EtOAc, 0.19 mmol) according to general procedure A. The crude product was purified by flash chromatography (12 g of silica gel, 0–20% MeOH/DCM gradient) to yield **2** (19 mg, 39%) as a white solid: ¹H NMR (400 MHz, DMSO-*d*₆) δ 13.25 (br s, 1H), 8.69 (s, 1H), 8.15 (s, 1H), 7.86 (s, 1H), 7.59 (d, *J* = 8.59 Hz, 1H), 7.55 (s, 1H), 7.39 (d, *J* = 8.59 Hz, 1H), 7.33 (d, *J* = 8.20 Hz, 1H), 6.96 (d, *J* = 8.20 Hz, 1H), 3.62–4.32 (m, 2H), 3.34–3.45 (m, 2H), 2.29 (s, 3H), 1.96–2.15 (m, 2H), 1.72–1.88 (m, 2H); *m/z* = 377.2 [M + H]⁺.

2'-tert-Butyl-1-(3,7-dimethyl-1H-indazole-5-carbonyl)-4',6'-dihydrospiro[piperidine-4,5'-pyrazolo[3,4-c]pyridin]-7'(2'H)-one (6). The title compound was prepared from 3,7-dimethyl-1H-indazole-5-carboxylic acid (**30**) (22 mg, 0.13 mmol), DMAP (4.7 mg, 0.04 mmol), T3P (0.10 mL, 50% in EtOAc, 0.15 mmol), Et₃N (0.11 mL, 0.76 mmol), and 2'-tert-butyl-4',6'-dihydrospiro[piperidine-4,5'-pyrazolo[3,4-c]pyridin]-7'(2'H)-one hydrochloride salt (**31**)¹⁹ (38 mg, 0.13 mmol) according to general procedure B. The resultant crude product was purified by flash chromatography (10 g silica gel, 1–10% MeOH/DCM gradient) to yield **6** (33 mg, 76%) as a white solid: ¹H NMR (400 MHz, CDCl₃) δ 10.93 (br s, 1H), 7.62 (s, 1H), 7.40 (s, 1H), 7.21 (s, 1H), 6.74 (br s, 1H), 3.76–4.12 (m, 2H), 3.64 (t, *J* = 10.2 Hz, 2H), 2.86 (s, 2H), 2.60 (s, 3H), 2.55 (s, 3H), 1.69–1.87 (m, 4H), 1.63 (s, 9H); *m/z* = 435.1 [M + H]⁺.

1-(3,7-Dimethyl-1H-indazole-5-carbonyl)-2'-isopropyl-4',6'-dihydrospiro[piperidine-4,5'-pyrazolo[3,4-c]pyridin]-7'(2'H)-one (7). The title compound was prepared from carboxylic acid **30** (22 mg, 0.13 mmol), DMAP (4.7 mg, 0.04 mmol), T3P (0.10 mL, 50% in EtOAc, 0.15 mmol), Et₃N (0.11 mL, 0.76 mmol), and 2'-isopropyl-4',6'-dihydrospiro[piperidine-4,5'-pyrazolo[3,4-c]pyridin]-7'(2'H)-one hydrochloride salt (**32**)²³ (38 mg, 0.13 mmol) according to general procedure B. The resultant crude product was purified by flash chromatography (10 g silica gel, 1–10% MeOH/DCM gradient) to yield **7** (31 mg, 76%) as a white solid: ¹H NMR (400 MHz, CDCl₃) δ 10.81 (br s, 1H), 7.59 (s, 1H), 7.24 (s, 1H), 7.18 (s, 1H), 6.77 (s, 1H), 4.55 (spt, *J* = 6.7 Hz, 1H), 3.62 (t, *J* = 10.1 Hz, 2H), 2.84 (s, 2H), 2.58 (s, 3H), 2.53 (s, 3H), 1.91–1.57 (m, 6H), 1.52 (d, *J* = 8.0 Hz, 6H); *m/z* = 421.3 [M + H]⁺.

2'-Cyclobutyl-1-(3,7-dimethyl-1H-indazole-5-carbonyl)-4',6'-dihydrospiro[piperidine-4,5'-pyrazolo[3,4-c]pyridin]-7'(2'H)-one (8). The title compound was prepared from 2'-cyclobutyl-4',6'-dihydrospiro[piperidine-4,5'-pyrazolo[3,4-c]pyridin]-7'(2'H)-one hydrochloride salt (**33**)²³ (20 mg, 0.060 mmol), carboxylic acid **30** (14 mg, 0.072 mmol), Et₃N (0.045 mL, 0.32 mmol), and T3P (0.07 mL of 50% in EtOAc, 0.1 mmol) using general procedure A via combinatorial chemistry (12.5 mg, 48%): *m/z* = 433.1 [M + H]⁺.

1-(3,7-Dimethyl-1H-indazole-5-carbonyl)-2'-(tert-pentyl)-4',6'-dihydrospiro[piperidine-4,5'-pyrazolo[3,4-c]pyridin]-7'(2'H)-one (9). The title compound was prepared from 2'-tert-pentyl-4',6'-dihydrospiro[piperidine-4,5'-pyrazolo[3,4-c]pyridin]-7'(2'H)-one hydrochloride salt (**34**)²³ (20 mg, 0.064 mmol), carboxylic acid **30** (15 mg, 0.077 mmol), Et₃N (0.045 mL, 0.32 mmol), and T3P (0.08 mL of 50% in EtOAc, 0.1 mmol) using general procedure A via combinatorial chemistry (12.9 mg, 45%): *m/z* = 449.2 [M + H]⁺.

1'-(tert-Butyl)-1-(3,7-dimethyl-1H-indazole-5-carbonyl)-4',6'-dihydrospiro[piperidine-4,5'-pyrazolo[3,4-c]pyridin]-7'(1'H)-one (10). The title compound was prepared from carboxylic acid **30** (24 mg, 0.13 mmol), DMAP (5 mg, 0.04 mmol), T3P (0.10 mL, 50% in EtOAc, 0.15 mmol), Et₃N (53 µL, 0.38 mmol), and 1'-tert-butyl-4',6'-dihydrospiro[piperidine-4,5'-pyrazolo[3,4-c]pyridin]-7'(1'H)-one hydrochloride salt (**35**)²³ (38 mg, 0.13 mmol) using general procedure B. The

crude material was purified by flash chromatography (10 g of silica gel, 1–10% MeOH/DCM gradient) to yield **10** (20 mg, 36%) as a white solid: ¹H NMR (400 MHz, CDCl₃) δ 10.34 (br s, 1H), 7.57 (s, 1H), 7.23 (s, 1H), 7.15 (s, 1H), 6.59 (br s, 1H), 3.68–3.59 (m, 4H), 2.83 (s, 2H), 2.55 (s, 3H), 2.49 (s, 3H), 1.86 (br s, 4H), 1.70 (s, 9H); *m/z* = 435.2 [M + H]⁺.

2'-(tert-Butyl)-6'-methyl-4',6'-dihydrospiro[piperidine-4,5'-pyrazolo[3,4-c]pyridin]-7'(2'H)-one hydrochloride salt (13). Intermediate **12**¹⁹ (235 mg, 0.65 mmol) was dissolved in DMF (8 mL) and cooled to 0 °C. Sodium hydride (78 mg, 60% in mineral oil, 1.9 mmol) was added, and the suspension was stirred in the ice bath for 10 min. MeI (0.12 mL, 1.9 mmol) was added, the ice bath was removed, and the reaction was stirred at rt for 4 h. The reaction mixture was diluted with water (50 mL), and the resulting suspension was extracted with MTBE (2 × 20 mL). The combined organics were washed with brine (50 mL), dried over Na₂SO₄, filtered, and concentrated under reduced pressure. The crude material was purified by flash chromatography (12 g silica gel, 20–100% EtOAc/heptane gradient) to yield the corresponding N-methylated lactam (209 mg, 86%) as a white solid: ¹H NMR (500 MHz, CDCl₃) δ ppm 7.35 (s, 1H), 4.07 (br s, 2H), 3.07 (s, 3H), 2.97 (s, 2H), 2.89 (br s, 2H), 1.95 (br s, 2H), 1.74–1.68 (m, 2H), 1.62 (s, 9H), 1.47 (s, 9H); *m/z* = 377.3 [M + H]⁺. The product isolated from the previous step (200 mg, 0.53 mmol) was suspended in EtOAc (5 mL) and treated with 4 N HCl in dioxane (1 mL). The reaction was stirred at rt for 18 h. Volatiles were removed under reduced pressure, and the resultant white solid was triturated with heptanes (10 mL) and concentrated to yield **13** (157 mg, 95%) as a white solid: ¹H NMR (500 MHz, DMSO-*d*₆) δ 9.40 (br s, 1H), 9.17 (br s, 1H), 7.69 (s, 1H), 3.20 (d, *J* = 12.44 Hz, 2H), 2.98–3.09 (m, 4H), 2.96 (s, 3H), 2.32 (dt, *J* = 4.27, 13.60 Hz, 2H), 1.68 (d, *J* = 13.66 Hz, 2H), 1.52 (s, 9H); *m/z* = 277.3 [M + H]⁺.

2'-(tert-Butyl)-1-(3,7-dimethyl-1H-indazole-5-carbonyl)-6'-methyl-4',6'-dihydrospiro[piperidine-4,5'-pyrazolo[3,4-c]pyridin]-7'(2'H)-one (14). The title compound was prepared from amine **13** (125 mg, 0.45 mmol), carboxylic acid **30** (86 mg, 0.45 mmol), Et₃N (0.10 mL, 0.90 mmol), and T3P (0.58 mL, 50% ethyl acetate, 0.87 mmol) according to general procedure A. The crude material was purified by flash chromatography (12 g of silica gel, 0–20% MeOH/DCM) to yield **14** (79 mg, 38%) as a white solid: ¹H NMR (500 MHz, DMSO-*d*₆) δ ppm 12.87 (s, 1H) 7.71 (s, 1H) 7.60 (s, 1H) 7.16 (s, 1H) 3.31 (s, 2H) 3.05 (br s, 2H) 2.96 (s, 3H) 2.45–2.52 (m, 10H) 1.85–2.00 (m, 2H) 1.52 (s, 9H); *m/z* = 449.4 [M + H]⁺.

2'-(tert-Butyl)-1-(3-(trifluoromethyl)-1H-indazole-5-carbonyl)-4',6'-dihydrospiro[piperidine-4,5'-pyrazolo[3,4-c]pyridin]-7'(2'H)-one (15). The title compound was prepared from amine **31**¹⁹ (28 mg, 0.083 mmol), 3-(trifluoromethyl)-1H-indazole-5-carboxylic acid (**36**) (19 mg, 0.083 mmol), Et₃N (0.035 mL, 0.25 mmol), and HATU (32 mg, 0.083 mmol) according to general procedure C via combinatorial chemistry (2.9 mg, 7%): *m/z* = 475.2 [M + H]⁺.

2'-(tert-Butyl)-1-(3-chloro-1H-indazole-5-carbonyl)-4',6'-dihydrospiro[piperidine-4,5'-pyrazolo[3,4-c]pyridin]-7'(2'H)-one (16). The title compound was prepared from amine **31**¹⁹ (50 mg, 0.15 mmol), 3-chloro-1H-indazole-5-carboxylic acid (**37**) (45 mg, 0.23 mmol), Et₃N (0.13 mL, 0.90 mmol), and T3P (0.18 mL of 50% in EtOAc, 0.30 mmol) using general procedure A via combinatorial chemistry (11.7 mg, 18%): *m/z* = 441.1 [M + H]⁺.

2'-(tert-Butyl)-1-(3-chloro-1H-indole-5-carbonyl)-4',6'-dihydrospiro[piperidine-4,5'-pyrazolo[3,4-c]pyridin]-7'(2'H)-one (17). The title compound was prepared from amine **31**¹⁹ (36 mg, 0.10 mmol), 3-chloro-1H-indole-5-carboxylic acid (**38**) (20 mg, 0.10 mmol), Et₃N (0.043 mL, 0.31 mmol), and HATU (39 mg, 0.10 mmol) according to general procedure C via combinatorial chemistry (18.7 mg, 42%): *m/z* = 440.1 [M + H]⁺.

2'-(tert-Butyl)-1-(3-chloro-1H-indole-6-carbonyl)-4',6'-dihydrospiro[piperidine-4,5'-pyrazolo[3,4-c]pyridin]-7'(2'H)-one (18). The title compound was prepared from amine **31**¹⁹ (36 mg, 0.10 mmol), 3-chloro-1H-indole-6-carboxylic acid (**39**) (20 mg, 0.10 mmol), Et₃N (0.043 mL, 0.31 mmol), and HATU (39 mg, 0.10 mmol) according to general procedure C via combinatorial chemistry (11.5 mg, 26%): *m/z* = 440.1 [M + H]⁺.

2'-(*tert*-Butyl)-1-(3-chloro-1*H*-pyrrolo[3,2-*b*]pyridine-6-carbonyl)-4',6'-dihydrospiro[piperidine-4,5'-pyrazolo[3,4-*c*]pyridin]-7'-(2'*H*)-one (**19**). The title compound was prepared from amine **31**¹⁹ (150 mg, 0.64 mmol), 3-chloro-1*H*-pyrrolo[3,2-*b*]pyridine-6-carboxylic acid (**40**) (220 mg, 0.66 mmol), EDC (156 mg, 0.77 mmol), HOBT (110 mg, 0.71 mmol), and Et₃N (0.45 mL, 3.2 mmol) according to general procedure D. The crude material was purified by flash chromatography (25 g of silica gel, 0–10% MeOH/DCM gradient) to yield **19** (190 mg, 67%) as a white solid: ¹H NMR (400 MHz, DMSO-*d*₆) δ 11.81 (d, *J* = 2.73 Hz, 1H), 8.42 (d, *J* = 1.76 Hz, 1H), 7.96 (d, *J* = 2.93 Hz, 1H), 7.84 (d, *J* = 1.76 Hz, 1H), 7.74–7.79 (m, 1H), 7.72 (s, 1H), 3.42–3.87 (m, 4H), 2.83 (s, 2H), 1.70–1.58 (m, 4H), 1.53 (s, 9H); *m/z* = 441.3 [M + H]⁺.

2'-(*tert*-Butyl)-1-(3-methoxyisoquinoline-6-carbonyl)-4',6'-dihydrospiro[piperidine-4,5'-pyrazolo[3,4-*c*]pyridin]-7'-(2'*H*)-one (**20**). 6-Bromo-3-methoxyisoquinoline (**41**)²³ (90 mg, 0.38 mmol) was placed into a microwave vial and dissolved in dioxane (6 mL). Amine **31**¹⁹ (244 mg, 0.727 mmol) and sodium acetate (131 mg, 1.5 mmol) were then added. Nitrogen was bubbled into the reaction for 15 min, Pd(dppf)Cl₂/DCM (102 mg, 0.125 mmol) was added, and carbon monoxide from a tank was bubbled in the reaction for 5 min. The reaction mixture was warmed to 80 °C in the microwave and left stirring for 8 h. The reaction was allowed to cool to rt and was diluted with EtOAc. The solids were filtered on a pad of Celite, and the solvent was removed under reduced pressure. This reaction was run via combinatorial chemistry, providing 4.1 mg (2%) of compound **20**: *m/z* = 448.1 [M + H]⁺.

2'-(*tert*-Butyl)-1-(2-methoxyquinoline-7-carbonyl)-4',6'-dihydrospiro[piperidine-4,5'-pyrazolo[3,4-*c*]pyridin]-7'-(2'*H*)-one (**21**). The title compound was prepared from 2-methoxyquinoline-7-carboxylic acid (**42**)²² (1.4 g, 6.8 mmol), amine **31**¹⁹ (2.7 g, 8.2 mmol), Et₃N (4.8 mL, 34 mmol), and T3P (4.7 mL of 50% in EtOAc, 7.1 mmol) according to general procedure A. The material was purified by flash chromatography (100 g silica gel, 2–20% MeOH/DCM) to provide **21** (2.94 g, 96%) as a white solid: ¹H NMR (400 MHz, CDCl₃) δ 8.00 (d, *J* = 8.97 Hz, 1H), 7.90 (s, 1H), 7.76 (d, *J* = 8.19 Hz, 1H), 7.41 (dd, *J* = 1.56, 8.19 Hz, 1H), 7.39 (s, 1H), 6.96 (d, *J* = 8.78 Hz, 1H), 6.18 (s, 1H), 4.09 (s, 3H), 3.41–3.75 (m, 4H), 2.86 (s, 2H), 1.70–1.99 (m, 4H), 1.62 (s, 9H); *m/z* = 448.5 [M + H]⁺.

2'-(*tert*-Butyl)-1-(1-methoxyisoquinoline-7-carbonyl)-4',6'-dihydrospiro[piperidine-4,5'-pyrazolo[3,4-*c*]pyridin]-7'-(2'*H*)-one (**22**). The title compound was prepared from 1-methoxyisoquinoline-7-carboxylic acid (**43**)²² (400 mg, 2.00 mmol), amine **31**¹⁹ (660 mg, 2.00 mmol), Et₃N (1.4 mL, 9.9 mmol), and T3P (1.36 mL of 50% in EtOAc, 2.04 mmol) according to general procedure A. The material was purified by flash chromatography (100 g silica gel, 2–20% MeOH/DCM gradient) to provide **22** (765 mg, 87%) as a white solid: ¹H NMR (400 MHz, CDCl₃) δ 8.28–8.33 (m, 1H), 8.06 (d, *J* = 5.85 Hz, 1H), 7.75–7.80 (m, 1H), 7.67–7.72 (m, 1H), 7.40 (s, 1H), 7.23 (d, *J* = 5.46 Hz, 1H), 6.20 (s, 1H), 4.14 (s, 3H), 3.99–4.12 (m, 1H), 3.59 (br s, 3H), 2.87 (s, 2H), 1.68–2.05 (m, 4H), 1.62 (s, 9H); *m/z* = 448.3 [M + H]⁺.

2'-(*tert*-Butyl)-1-[(2-(methylamino)quinolin-7-yl)carbonyl]-2',4'-dihydrospiro[piperidine-4,5'-pyrazolo[3,4-*c*]pyridin]-7'-(6'*H*)-one (**23**). The title compound was prepared from amine **31**¹⁹ (87 mg, 0.25 mmol), 2-(methylamino)quinoline-7-carboxylic acid²³ (50 mg, 0.26 mmol), Et₃N (0.11 mL, 0.74 mmol), HOBT (40 mg, 0.30 mmol), and EDC (52 mg, 0.27 mmol) using general procedure D. The crude material was purified by flash chromatography (12 g silica gel, 0–10% MeOH/DCM gradient) to provide **23** (84 mg, 76%) as a white powder: ¹H NMR (400 MHz, DMSO-*d*₆) δ 7.82 (d, *J* = 8.97 Hz, 1H), 7.72 (s, 1H), 7.63 (d, *J* = 8.04 Hz, 1H), 7.66 (br s, 1H), 7.39–7.43 (m, 1H), 7.08–7.13 (m, 1H), 7.06 (dd, *J* = 8.10, 1.66 Hz, 1H), 6.75 (d, *J* = 8.97 Hz, 1H), 3.77 (br s, 1H), 3.58 (br s, 1H), 3.46 (br s, 1H), 3.34 (br s, 1H), 2.87 (d, *J* = 4.68 Hz, 3H), 2.80 (br s, 2H), 1.55–1.77 (m, 4H), 1.49 (s, 9H); *m/z* = 447.4 [M + H]⁺.

2'-(*tert*-Butyl)-1-(1-(methylamino)isoquinoline-7-carbonyl)-4',6'-dihydrospiro[piperidine-4,5'-pyrazolo[3,4-*c*]pyridin]-7'-(2'*H*)-one (**24**). The title compound was prepared from amine **31**¹⁹ (657 mg, 2.00 mmol), 1-(methylamino)isoquinoline-7-carboxylic acid (**44**)²² (360 mg, 1.78 mmol), Et₃N (1.5 mL, 11 mmol), DMAP (4.5 mg,

0.033 mmol), and T3P (1.6 mL, 50% in EtOAc, 2.7 mmol) according to general procedure B. The crude material was purified by flash chromatography (40 g of silica gel, 0–20% MeOH/EtOAc gradient) to provide **24** (294 mg, 40%) as a white solid: ¹H NMR (400 MHz, DMSO-*d*₆) δ 8.23 (s, 1H), 7.92 (d, *J* = 5.87 Hz, 1H), 7.69–7.78 (m, 3H), 7.57 (dd, *J* = 8.31, 1.47 Hz, 2H), 6.89 (d, *J* = 5.87 Hz, 1H), 3.33–3.85 (m, 4H), 2.95 (d, *J* = 4.30 Hz, 3H), 2.82 (s, 2H), 1.55–1.79 (m, 4H), 1.52 (s, 9H); *m/z* = 447.4 [M + H]⁺.

2'-(*tert*-Butyl)-1-(2-chloroquinoline-7-carbonyl)-4',6'-dihydrospiro[piperidine-4,5'-pyrazolo[3,4-*c*]pyridin]-7'-(2'*H*)-one (**25**). The title compound was prepared from amine **31**¹⁹ (1.19 g, 3.54 mmol), 2-chloroquinoline-7-carboxylic acid (**45**) (700 mg, 3.37 mmol), Et₃N (1.9 mL, 14 mmol), HOBT (547 mg, 4.05 mmol), and EDC (776 mg, 4.05 mmol) according to general procedure D. The crude material was purified by flash chromatography (100 g of silica gel, 0–20% MeOH/DCM gradient) to provide **25** (1.5 g, quant.) as a white solid: ¹H NMR (400 MHz, CDCl₃) δ 8.12 (d, *J* = 8.36 Hz, 1H), 7.98 (br s, 1H), 7.88 (dd, *J* = 8.36 Hz, 1H), 7.61 (dd, *J* = 8.36, 1.59 Hz, 1H), 7.44 (d, *J* = 1.59 Hz, 1H), 7.39 (s, 1H), 5.91 (br s, 1H), 4.06–4.22 (m, 1H), 3.38–3.64 (m, 3H), 2.85 (br s, 2H), 1.67–1.97 (m, 4H), 1.61 (s, 9H); *m/z* = 452.3 [M + H]⁺.

2'-(*tert*-Butyl)-1-(2-(propylamino)quinoline-7-carbonyl)-4',6'-dihydrospiro[piperidine-4,5'-pyrazolo[3,4-*c*]pyridin]-7'-(2'*H*)-one (**26**). A mixture of chloroquinoline **25** (100 mg, 0.221 mmol) and *n*-propylamine (13.1 mg, 0.221 mmol) was heated in a sealed vial at 80 °C for 18 h. The reaction mixture was concentrated to dryness and the crude product was purified by flash chromatography (12 g silica gel, 0–10% MeOH/DCM gradient) to provide **26** (82 mg, 78%) as a white foam: ¹H NMR (400 MHz, CDCl₃) δ 7.79 (d, *J* = 8.81 Hz, 1H), 7.61–7.62 (m, 1H), 7.59 (d, *J* = 8.21 Hz, 1H), 7.37 (s, 1H), 7.19 (dd, *J* = 8.17, 1.57 Hz, 1H), 6.65 (d, *J* = 8.81 Hz, 1H), 5.79 (s, 1H), 4.69–4.73 (m, 1H), 4.00–4.15 (m, 1H), 3.41–3.63 (m, 5H), 2.83 (s, 2H), 1.64–1.92 (m, 6H), 1.61 (s, 9H), 1.02 (t, *J* = 7.41 Hz, 3H); *m/z* = 475.6 [M + H]⁺.

2'-(*tert*-Butyl)-1-(2-(dimethylamino)quinoline-7-carbonyl)-4',6'-dihydrospiro[piperidine-4,5'-pyrazolo[3,4-*c*]pyridin]-7'-(2'*H*)-one (**27**). A mixture of chloroquinoline **25** (100 mg, 0.221 mmol) and dimethylamine (2.2 mL, 4.4 mmol) was heated in a sealed vial at 80 °C for 18 h. The reaction mixture was then concentrated to dryness, and the crude product was purified by flash chromatography (12 g of silica gel, 0–10% MeOH/DCM gradient) to provide **27** (30.3 mg, 30%) as a white foam: ¹H NMR (400 MHz, CDCl₃) δ 7.87 (d, *J* = 9.17 Hz, 1H), 7.69 (br s, 1H), 7.62 (d, *J* = 8.00 Hz, 1H), 7.39 (s, 1H), 7.17–7.22 (m, 1H), 6.94 (d, *J* = 9.17 Hz, 1H), 5.82 (s, 1H), 4.08 (s, 1H), 3.45–3.68 (m, 3H), 3.25 (s, 6H), 2.86 (s, 2H), 1.70–1.99 (m, 4H), 1.63 (s, 9H); *m/z* = 461.4 [M + H]⁺.

■ ASSOCIATED CONTENT

Supporting Information

Experimental details for the synthesis of key intermediates as well as compounds **1**–**27**. This material is available free of charge via the Internet at <http://pubs.acs.org>.

■ AUTHOR INFORMATION

Corresponding Author

*Tel: 617-551-3302. E-mail: kim.huard@pfizer.com.

Notes

The authors declare no competing financial interest.

■ ACKNOWLEDGMENTS

The authors would like to thank Kristen Ford, Kristin L. Rockwell, and Fabien Vincent for their work on the biological screening, Margaret S. Landis and Brenda Ramos for the formulation work, and Mark Niosi for his work on the pharmacokinetic studies.

■ ABBREVIATIONS

T2DM, type 2 diabetes mellitus; DNL, *de novo* lipogenesis; ACC, acetyl-CoA carboxylase; CPT-I, carnitine palmitoyltransferase 1; LipE, lipophilic ligand efficiency; HLM, human liver microsome; CYP, cytochrome P450; NaH, sodium hydride; MeI, iodomethane; HCl, hydrochloric acid; T3P, propylphosphonic anhydride; Et₃N, triethylamine; HOBt, *N*-hydroxybenzotriazole; EDC, 1-ethyl-3-(3-dimethylaminopropyl)-carbodiimide; C_{max} , maximum concentration; AUC, area under the curve; SEDDS, self-emulsifying drug delivery system; ESI-MS, electrospray ionization coupled with mass spectrometry; HPLC, high-performance liquid chromatography; TFA, trifluoroacetic acid; MeCN, acetonitrile; DMSO, dimethylsulfoxide; HEPES, 4-(2-hydroxyethyl)-1-piperazineethanesulfonic acid; DTT, dithiothreitol; BSA, bovine serum albumin; LSC, liquid scintillation counting; NaOH, sodium hydroxide; DMF, *N,N*-dimethylformamide; rt, room temperature; DCM, dichloromethane; DMAP, *N,N*-dimethyl-4-aminopyridine; MTBE, methyl *tert*-butyl ether

■ REFERENCES

- (1) Savage, D. B.; Petersen, K. F.; Shulman, G. I. Disordered Lipid Metabolism and the Pathogenesis of Insulin Resistance. *Physiol. Rev.* **2007**, *87*, 507–520.
- (2) (a) Hwang, J.-H.; Stein, D. T.; Barzilai, N.; Cui, M.-H.; Tonelli, J.; Kishore, P.; Hawkins, M. Increased Intrahepatic Triglyceride Is Associated with Peripheral Insulin Resistance: *In Vivo* MR Imaging and Spectroscopy Studies. *Am. J. Physiol. Endocrinol. Metab.* **2007**, *293*, E1663–E1669. (b) Korenblat, K. M.; Fabbrini, E.; Mohammed, B. S.; Klein, S. Liver, Muscle, and Adipose Tissue Insulin Action Is Directly Related to Intrahepatic Triglyceride Content in Obese Subjects. *Gastroenterology* **2008**, *134*, 1369–1375.
- (3) Krssak, M.; Peterson, K. F.; Dresner, A.; DiPietro, L.; Vogel, S. M.; Rothman, D. L.; Shulman, G. I.; Roden, M. Intramyocellular Lipid Concentrations are Correlated with Insulin Sensitivity in Humans: A ¹H NMR Spectroscopy Study. *Diabetologia* **1999**, *42*, 113–116.
- (4) Choi, C. S.; Savage, D. B.; Abu-Eliga, L.; Liu, Z.-X.; Kim, S.; Kulkarni, A.; Distefano, A.; Hwang, Y.-J.; Reznick, R. M.; Codella, R.; Zhang, D.; Cline, G. W.; Wakil, S. J.; Shulman, G. I. Continuous Fat Oxidation in Acetyl-CoA Carboxylase 2 Knockout Mice Increases Total Energy Expenditure, Reduces Fat Mass, and Improves Insulin Sensitivity. *Proc. Natl. Acad. Sci. U.S.A.* **2007**, *104*, 16480–16485.
- (5) Savage, D. B.; Choi, C. S.; Samuel, V. T.; Liu, Z.-X.; Zhang, D.; Wang, A.; Zhang, X.-M.; Cline, G. W.; Yu, X. X.; Geisler, J. G.; Bhanot, S.; Monia, B. P.; Shulman, G. I. Reversal of Diet-Induced Hepatic Steatosis and Hepatic Insulin Resistance by Antisense Oligonucleotide Inhibitors of Acetyl-CoA Carboxylases 1 and 2. *J. Clin. Invest.* **2006**, *116*, 817–824.
- (6) (a) Harwood, H. J., Jr.; Petras, S. F.; Shelly, L. D.; Zaccaro, L. M.; Perry, D. A.; Makowski, M. R.; Hargrove, D. M.; Martin, K. A.; Tracey, W. R.; Chapman, J. G.; Magee, W. P.; Dalvie, D. K.; Soliman, V. F.; Martin, W. H.; Mularski, C. J.; Eisenbeis, S. A. Isozyme-nonspecific *N*-Substituted Bipiperidylcarboxamide Acetyl-CoA Carboxylase Inhibitors Reduce Tissue Malonyl-CoA Concentrations, Inhibit Fatty Acid Synthesis, and Increase Fatty Acid Oxidation in Cultured Cells and in Experimental Animals. *J. Biol. Chem.* **2003**, *278*, 37099–37111. (b) Schreurs, M.; van Dijk, T. H.; Gerding, A.; Havinga, R.; Reijngoud, D.-J.; Kuipers, F. Soraphen, an Inhibitor of the Acetyl-CoA Carboxylase System, Improves Peripheral Insulin Sensitivity in Mice Fed a High-Fat Diet. *Diabetes, Obes. Metab.* **2009**, *11*, 987–991.
- (7) Kusunoki, J.; Kanatani, A.; Moller, D. E. Modulation of Fatty Acid Metabolism as a Potential Approach to the Treatment of Obesity and the Metabolic Syndrome. *Endocrine* **2006**, *29*, 91–100.
- (8) Corbett, J. W.; Freeman-Cook, K. D.; Elliott, R.; Vajdos, F.; Rajamohan, F.; Kohls, D.; Marr, E.; Zhang, H.; Tong, L.; Tu, M.; Murdande, S.; Doran, S. D.; Houser, J. A.; Song, W.; Jones, C. J.; Coffey, S. B.; Buzon, L.; Minich, M. L.; Dirico, K. J.; Tapley, S.; McPherson, R. K.; Sugarman, E.; Harwood, H. J., Jr.; Esler, W. Discovery of Small Molecule Isozyme Non-Specific Inhibitors of Mammalian Acetyl-CoA Carboxylase 1 and 2. *Bioorg. Med. Chem. Lett.* **2010**, *20*, 2383–2388.
- (9) Freeman-Cook, K. D.; Amor, P.; Bader, S.; Buzon, L. M.; Coffey, S. B.; Corbett, J. W.; Dirico, K. J.; Doran, S. D.; Elliott, R. L.; Esler, W.; Guzman-Perez, A.; Henegar, K. E.; Houser, J. A.; Jones, C. S.; Limberakis, C.; Loomis, K.; McPherson, K.; Murdande, S.; Nelson, K. L.; Phillion, D.; Pierce, B. S.; Sugarman, E.; Tapley, S.; Tu, M.; Zhao, Z. Maximizing Lipophilic Efficiency: The Use of Free-Wilson Analysis in the Design of Inhibitors of Acetyl-CoA Carboxylase. *J. Med. Chem.* **2012**, *55*, 935–942.
- (10) Experimental details for the assay used to determine IC₅₀ values are reported in the Experimental Section.
- (11) Edwards, M. P.; Price, D. A. Role of Physicochemical Properties and Ligand Lipophilicity Efficiency in Addressing Drug Safety Risks. *Annu. Rep. Med. Chem.* **2010**, *45*, 380–391.
- (12) Lombardo, F.; Shalaeva, M. Y.; Tupper, K. A.; Gao, F. ElogD_{oct}: A Tool for Lipophilicity Determination in Drug Discovery. *J. Med. Chem.* **2001**, *44*, 2490–2497.
- (13) Obach, R. S. The Prediction of Human Clearance from Hepatic Microsomal Metabolism Data. *Curr. Opin. Drug Discovery Dev.* **2001**, *4*, 36–44.
- (14) Di, L.; Whitney-Pickett, C.; Umland, J. O.; Zhang, H.; Zhang, X.; Gebhard, D. F.; Lai, Y.; Federico, J. J.; Davidson, R. E.; Smith, R.; Reyner, E. L.; Lee, C.; Feng, B.; Rotter, C.; Varma, M. V.; Kempshall, S.; Fenner, K.; El-Kattan, A. F.; Liston, T. E.; Troutman, M. D. Development of a New Permeability Assay Using Low-Efflux MDCKII Cells. *J. Pharm. Sci.* **2011**, *100*, 4974–4985.
- (15) Eng, H.; Niosi, M.; Tan, B.; Doran, S.; Garcia-Irizarry, C. N.; Griffith, D. A.; Kalgutkar, A. S.; Kung, D. W.; Esler, W.; Steidl, J., unpublished results.
- (16) Limberakis, C.; Li, J.; Balan, G.; Griffith, D. A.; Kung, D. W.; Rose, C.; Vrieze, D. Complementary α -Alkylation Approaches for a Sterically Hindered Spiro[pyrazolopyranpiperidine]ketone. *Tetrahedron Lett.* **2012**, *53*, 2543–2547.
- (17) Compound **2** was prepared by condensation of *N*-protected 4-piperidinone with salicylamide under previously reported conditions: Gammill, R. B. A New Amine Catalyzed Synthesis of 2-Substituted 2,3-Dihydro-4H-1,3-benzoxazin-4-ones. *J. Org. Chem.* **1981**, *46*, 3340–3342. See Supporting Information for more details.
- (18) For examples of aminor ACC inhibitors, see: Anderson, R.; Breazeale, S.; Elich, T.; Lee, S.-F. Modulators of acetyl-coenzyme A carboxylase and methods of use thereof. U.S. Patent US20100009982, 2010.
- (19) For experimental details and synthesis of compounds **5**, **11**, **12**, and **31**, see Huard, K.; Bagley, S. W.; Menhaji-Klotz, E.; Prévile, C.; Southers, J. A.; Smith, A. C.; Edmonds, D. J.; Lucas, J. C.; Dunn, M. F.; Allanson, N. M.; Blaney, E. L.; Garcia-Irizarry, C. N.; Kohrt, J. T.; Griffith, D. A.; Dow, R. L. Synthesis of Spiropiperidine Lactam Acetyl-CoA Carboxylase Inhibitors. *J. Org. Chem.* **2012**, *77*, 10050–10057.
- (20) Compound **6** was tested for cytochrome P450 time-dependant inhibition at 60 μ M in human liver microsomes and caused a 38% decrease activity of CYP3A4 after 30 minutes of incubation, as determined by midazolam metabolism. Other examples of formation of reactive metabolites associated with 3-methylindazole scaffold were previously reported in the literature: Jones, L. H.; Allan, G.; Barba, O.; Burt, C.; Corbau, R.; Dupont, T.; Knöchel, T.; Irving, S.; Middleton, D. S.; Mowbray, C. E.; Perros, M.; Ringrose, H.; Swain, N. A.; Webster, R.; Westby, M.; Phillips, C. Novel Indazole Non-Nucleoside Reverse Transcriptase Inhibitors Using Molecular Hybridization Based on Crystallographic Overlays. *J. Med. Chem.* **2009**, *52*, 1219–1223.
- (21) IC₅₀ values for ACC1 and ACC2 were obtained using a radiometric assay, as described in the Experimental Section and are reported as the geometric mean based on $n \geq 3$ (except for compound **5**, $n = 1$). Compounds **1**, **5**, and **6** were also compared using a previously reported assay format (see ref 9). IC₅₀ values ($n \geq 3$) for

ACC1 and ACC2, respectively, were as follows: **1** (111 ± 21 nM, 11 ± 1 nM); **5** (164 ± 40 nM, 67 ± 35 nM); **6** (7 ± 1 nM, 2.1 ± 0.6 nM).

(22) The synthesis of 6-methylspiro[1,3-benzoxazine-2,4'-piperidin]-4(3*H*)-one hydrochloride salt (**28**), 2-methoxyquinoline-7-carboxylic acid (**42**), 1-methoxyisoquinoline-7-carboxylic acid (**43**), and 1-(methylamino)isoquinoline-7-carboxylic acid (**44**) is described in the Supporting Information.

(23) The synthesis of 2'-isopropyl-4',6'-dihydrospiro[piperidine-4,5'-pyrazolo[3,4-*c*]pyridin]-7'(2'*H*)-one hydrochloride salt (**32**), 2'-cyclobutyl-4',6'-dihydrospiro[piperidine-4,5'-pyrazolo[3,4-*c*]pyridin]-7'(2'*H*)-one hydrochloride salt (**33**), 2'-*tert*-pentyl-4',6'-dihydrospiro[piperidine-4,5'-pyrazolo[3,4-*c*]pyridin]-7'(2'*H*)-one hydrochloride salt (**34**), 1'-*tert*-butyl-4',6'-dihydrospiro[piperidine-4,5'-pyrazolo[3,4-*c*]pyridin]-7'(1'*H*)-one hydrochloride salt (**35**), 6-bromo-3-methoxyisoquinoline (**41**), and 2-(methylamino)quinoline-7-carboxylic acid was previously described in the literature: Bagley, S. W.; Dow, R. L.; Griffith, D. A.; Smith, A. C. N1/N2-Lactam Acetyl-CoA Carboxylase Inhibitors. International Patent WO12056372; 2012.